PHYSICAL REVIEW B **84**, 020403(R) (2011)

Theory of resonant inelastic x-ray scattering in iridium oxide compounds: Probing spin-orbit-entangled ground states and excitations

Luuk J. P. Ament,[1,2] Giniyat Khaliullin,[3] and Jeroen van den Brink[2]
[1]*Institute-Lorentz for Theoretical Physics, Universiteit Leiden, NL-2300 RA Leiden, The Netherlands*
[2]*Institute for Theoretical Solid State Physics, IFW Dresden, D-01171 Dresden, Germany*
[3]*Max-Planck-Institut für Festkörperforschung, Heisenbergstrasse 1, D-70569 Stuttgart, Germany*
(Received 28 August 2010; revised manuscript received 10 June 2011; published 12 July 2011)

We determine how the elementary excitations of iridium-oxide materials, which are dominated by a strong relativistic spin-orbit coupling, appear in resonant inelastic x-ray scattering (RIXS). Whereas the RIXS spectral weight at the L_2 x-ray edge vanishes in the limit of cubic symmetry, we find it to be strong at the L_3 edge. Applying this to Sr_2IrO_4, we observe that RIXS, besides being sensitive to local doublet-to-quartet transitions, meticulously maps out the strongly dispersive delocalized excitations of the low-lying spin-orbit doublets.

DOI: 10.1103/PhysRevB.84.020403 PACS number(s): 75.25.Dk, 78.70.Ck, 71.70.Ej, 75.30.Et

Materials containing ions with an orbital degeneracy show a plethora of physical effects related to the spontaneous lifting of this degeneracy.[1] The two degeneracy-breaking mechanisms in Mott insulators traditionally considered are the cooperative Jahn-Teller effect,[2] involving a change in lattice symmetry, and the superexchange interactions,[3] intertwining long-range ordering of orbital and magnetic degrees of freedom. A third and less explored possibility exists in systems containing heavy ions, where strong relativistic spin-orbit coupling dominates the spin-orbital physics.[4]

The strong spin-orbit interaction can cause entirely different kinds of ordering that are of topological nature. This was recently proposed for certain iridium oxides,[5,6] members of a large family of iridium-based materials. Na_2IrO_3, for instance, is predicted to be a topological insulator exhibiting the quantum spin Hall effect at room temperature.[5] This system can also be described in terms of a Mott insulator, with interactions between the effective iridium spin-orbital degrees of freedom governed by the Kitaev-Heisenberg model.[7–9] In the pyrochlore iridates $A_2Ir_2O_7$ (where A is a 3+ ion), a quantum phase transition from a topological band insulator to a topological Mott insulator has been proposed as a function of the electron-electron interaction strength.[6,10,11]

To establish whether and how such phases are realized in iridium oxides, it is essential to probe and understand their spin-orbital ordering and in particular the elementary excitations emergent from the interplay between electronic correlations, band behavior, and strong spin-orbit coupling. Knowledge of excitations is essential to gain understanding of the dynamical properties of the potentially unique states of matter that can be realized in iridates. It forms the cornerstone for the development of realistic model Hamiltonians for iridates, and can spark an interplay between theory and experiment of an intensity that has been lacking so far. In this context it is advantageous to consider the structurally less complicated, single-layer iridium perovskite Sr_2IrO_4. This material is in many respects the analog of the high-T_c cuprate parent compound La_2CuO_4.[8] Structurally it is identical, with the obvious difference that the Ir $5d$ valence electrons are, as opposed to the Cu $3d$ electrons, very strongly spin-orbit coupled. The similarity cuts deeper, however, as the low-energy sector of the iridates is spanned by local spin-orbit doublets with an effective spin of $1/2$, which reside on a square lattice and interact via superexchange—a close analogy with the undoped cuprates. This observation motivates doping studies of Sr_2IrO_4 searching for superconductivity.[12,13]

Experimentally far less is known about the microscopic ordering and excitations in iridates than in cuprates. Inelastic neutron scattering, which can in principle reveal such properties, is not possible because Ir is a strong neutron absorber.[14] As a consequence, not even the interaction strength between the effective spins in the simplest iridium oxides is established: Estimates for Sr_2IrO_4, for instance, range from $\sim$50 meV (Ref. 8) to $\sim$110 meV.[15]

Here we show that while for iridates neutron scattering falls short, photon-in photon-out scattering in the form of resonant inelastic x-ray scattering (RIXS)[16] fills the void: RIXS at the iridium L edge offers direct access to the excitation spectrum across the Brillouin zone, enabling one to measure the dispersion of elementary magnetic excitations. We develop the theoretical description of RIXS for iridates in general, which we then apply to Sr_2IrO_4. We demonstrate explicitly how, besides the low-energy magnons related to long-range order of the doublets, RIXS will also reveal the dynamics of higher-energy, doublet-to-quartet, spin-orbit excitations. Such observations allow to directly test theoretical models and to develop and refine model Hamiltonian descriptions for iridates systems by, for instance, extracting accurate values of the superexchange and spin-orbit coupling constants J and λ, respectively.

Ir^{4+} ionic ground state. In the iridium-oxides Ir^{4+} ions are located in octahedra of oxygen ions, splitting the $5d$ levels by $\sim$3 eV into e_g and t_{2g} orbitals.[17] Because this crystal-field splitting is an order of magnitude larger than the spin-orbit coupling λ, the t_{2g} levels do not hybridize much with the e_g orbitals, and a t_{2g}^5 configuration is established.[18] The symmetry of the t_{2g}^5 ground state is in principle governed by three factors: superexchange interactions, additional lattice-induced crystal-field splittings, and relativistic spin-orbit coupling.[19] The superexchange J (Ref. 8) is estimated to be approximately an order of magnitude smaller than $\lambda \approx 0.4$ eV.[20] An elongation of the octahedra along the z axis[21] favors a ground state where the hole is in the xy orbital. But experimental data strongly

 ©2011 American Physical Society

favor the spin-orbit coupling scenario over the lattice splitting scenario, however.[4,18]

The orbital degree of freedom of the hole can be described by an effective angular momentum $l = 1$, related to the true orbital angular momentum by $\mathbf{l} = -\mathbf{L}$.[22] The orbital eigenstates of l_z are described by the annihilation operators $d_{0,\pm1}$, defined in terms of the real t_{2g} wave functions by the relations $d_{yz} = -(d_1 - d_{-1})/\sqrt{2}$, $d_{zx} = i(d_1 + d_{-1})/\sqrt{2}$, $d_{xy} = d_0$. When the spin-orbit coupling term is projected to the t_{2g} subspace, it becomes $-\lambda \mathbf{l}\cdot\mathbf{S}$. Tetragonal lattice distortions can also be included, and the Hamiltonian for a single Ir ion is[8] $H = -\lambda \mathbf{l}\cdot\mathbf{S} - \Delta l_z^2$, with $\Delta > 0$ for elongation along the z axis. The six eigenstates group into three Kramers doublets, described by the fermions f, g, and h with annihilation operators

$$\begin{aligned} f_\uparrow &= \sin\theta\, d_{0\uparrow} - \cos\theta\, d_{1\downarrow}, & g_\uparrow &= d_{1\uparrow}, \\ f_\downarrow &= \cos\theta\, d_{-1\uparrow} - \sin\theta\, d_{0\downarrow}, & g_\downarrow &= d_{-1\downarrow}, \\ h_\uparrow &= \cos\theta\, d_{0\uparrow} + \sin\theta d_{1\downarrow}, \\ h_\downarrow &= \cos\theta\, d_{0\downarrow} + \sin\theta d_{-1\uparrow}, \end{aligned} \tag{1}$$

and with energies $\omega_f = \lambda/(\sqrt{2}\tan\theta)$, $\omega_g = -\Delta - \lambda/2$ and $\omega_h = -(\lambda\tan\theta)/\sqrt{2}$, where $\tan 2\theta = 2\sqrt{2}\lambda/(\lambda - 2\Delta)$. For $\Delta = 0$, which corresponds to the cubic, isotropic situation $\sin\theta = \sqrt{1/3}$ and $\cos\theta = \sqrt{2/3}$. For $\lambda/\Delta \ll 1$, the hole's ground-state doublet is $\{|xy\uparrow\rangle, |xy\downarrow\rangle\}$. For $\lambda/\Delta \gg 1$, the eigenstates are characterized by the total effective angular momentum $\mathbf{J}_{\rm eff} = \mathbf{l} + \mathbf{S}$. In the ground state, the hole occupies the f doublet ($J_{\rm eff} = 1/2$), which is separated by an energy of $3\lambda/2$ from the $J_{\rm eff} = 3/2$ quartet, which splits into the g and h doublets.

The remaining twofold ground-state degeneracy cannot be removed by Jahn-Teller distortions because the two states of the Kramers doublet have exactly the same charge distribution. Superexchange coupling, however, is present in all iridates, and couples the local doublets, thus dictating the low energy collective dynamics of the material.

RIXS cross section. RIXS is particularly suited to probe higher-energy magnetic excitations and dispersions, as demonstrated in the cuprates.[23–26] In RIXS,[16,27] a photon with momentum $\hbar\mathbf{k}$, energy $\omega_{\mathbf{k}}$, and polarization $\boldsymbol{\epsilon}$ is scattered to $\hbar\mathbf{k}'$, $\omega_{\mathbf{k}'}$, and $\boldsymbol{\epsilon}'$, losing momentum $\hbar\mathbf{q} = \hbar\mathbf{k} - \hbar\mathbf{k}'$ and energy $\omega = \omega_{\mathbf{k}} - \omega_{\mathbf{k}'}$ to the sample. $\omega_{\mathbf{k}}$ is tuned to a certain atomic resonance of the material under study, greatly enhancing the scattering cross section. In our case, that will be the Ir L edge: The $2p$ core electron is excited into the empty $5d$ t_{2g} state. After a very short time, another electron from the t_{2g} levels can fall back to the core hole under the emission of an outgoing x ray. The system is left in an excited state, whose energy and momentum are taken from the scattered x-ray photon, which is measured.

The RIXS cross section is described by the Kramers-Heisenberg equation,[28] where the photon absorption and subsequent emission are governed by the dipole operator $\mathcal{D} = \sum_{\mathbf{R}} e^{i\mathbf{k}\cdot\mathbf{R}}\, \mathbf{r}\cdot\boldsymbol{\epsilon}$ acting on all electrons of an Ir^{4+} ion at site $\mathbf{R}$. The phonon polarization is $\boldsymbol{\epsilon}$.

The intermediate state has a filled shell ($5d$ t_{2g}^6), so the dominant multiplet effect comes from the core orbital's spin-orbit coupling Λ: The $2p$ core states split into $J = 1/2$ (the L_2 edge) and $J = 3/2$ states (the L_3 edge). Since the L_2 and the L_3 edge are separated by 1.6 keV,[4] their interference is negligible, given the much smaller lifetime broadening of a few eV.[29] Because the $2p$ core states have the same angular momenta as the $5d$ t_{2g} states, we can describe them with the three fermions F, G, and H, analogous to Eq. (1), where we replace (d_{yz}, d_{zx}, d_{xy}) by (p_x, p_y, p_z) and the parameters λ, Δ, and θ by Λ, δ, and Θ. The tetragonal distortion δ is expected to be very small for the deep $2p$ core states.

The lifetime broadening at the Ir L edge is still quite large compared to the dynamics of the $5d$ electrons.[18,29] Therefore, we make the fast collision approximation $E_i + \hbar\omega_{\mathbf{k}} - E_n + i\Gamma \approx i\Gamma$.[30] The sum over n in the Kramers-Heisenberg equation can be performed, and comprises the core states of either the L_2 or the L_3 edge. In second quantization, the dipole operators are $\mathbf{r}\cdot\boldsymbol{\epsilon} = \sum_{\alpha,\beta,\sigma} \langle 5d_\alpha|\mathbf{r}|2p_\beta\rangle \cdot \boldsymbol{\epsilon}\, d^\dagger_{\alpha\sigma}\, p_{\beta\sigma} +$ H.c. which can be denoted as $(D_2 + D_3) +$ H.c., where $D_{2,3}$ are the local dipole transition operators for the L_2 and L_3 edge, respectively. The RIXS amplitude becomes $A_{\mathbf{q}} \propto \langle f| \sum_{\mathbf{R}} e^{i\mathbf{q}\cdot\mathbf{R}} [D^\dagger(\boldsymbol{\epsilon}'^*) D(\boldsymbol{\epsilon})]_{\mathbf{R}} |0\rangle$, where $\mathbf{R}$ runs over all Ir sites and the RIXS intensity $I_{\mathbf{q}}(\omega) = \sum_f |A_{\mathbf{q}}|^2 \delta(\omega - E_f)$. Integrating out the core hole degrees of freedom, we obtain the following inelastic scattering operator:

$$\begin{aligned} D^\dagger D = \sum_{\sigma\in\{\uparrow,\downarrow\}} \big[& B^{ff}_{\sigma\sigma} f^\dagger_\sigma f_\sigma + B^{ff}_{\sigma\bar\sigma} f^\dagger_\sigma f_{\bar\sigma} + B^{fg}_{\sigma\sigma} f^\dagger_\sigma g_\sigma \\ & + B^{fg}_{\sigma\bar\sigma} f^\dagger_\sigma g_{\bar\sigma} + B^{fh}_{\sigma\sigma} f^\dagger_\sigma h_\sigma + B^{fh}_{\sigma\bar\sigma} f^\dagger_\sigma h_{\bar\sigma} \big]. \end{aligned} \tag{2}$$

At the L_2 edge, the intradoublet scattering matrix elements $B^{ff}_{\sigma\sigma} = -\sin^2(\theta - \Theta)\epsilon'^*_{\bar\sigma}\epsilon_{\bar\sigma}$ and $B^{ff}_{\sigma\bar\sigma} = 0$. The doublet-quartet excitation matrix elements of the spin-orbit multiplet are $B^{fg}_{\sigma\sigma} = \sin(\theta - \Theta)\cos\Theta\ \epsilon'^*_{\bar z}\epsilon_{\bar\sigma}$, $B^{fg}_{\sigma\bar\sigma} = -(-1)^\sigma \sin(\theta - \Theta)\sin\Theta\ \epsilon'^*_\sigma\epsilon_{\bar\sigma}$, $B^{fh}_{\sigma\sigma} = -\frac{1}{2}(-1)^\sigma \sin 2(\theta - \Theta)\epsilon'^*_{\bar\sigma}\epsilon_{\bar\sigma}$, and $B^{fh}_{\sigma\bar\sigma} = 0$, where $(-1)^\sigma$ is 1 for $\sigma = \uparrow$ and -1 for $\sigma = \downarrow$. Further, $\epsilon_\uparrow = \epsilon_+$ and $\epsilon_\downarrow = \epsilon_-$, with $\epsilon_\pm = (\epsilon_x \pm i\epsilon_y)/\sqrt{2}$. In the case of dominant spin-orbit coupling, $\theta = \Theta$. Since all matrix elements at the L_2 edge are proportional to $\sin(\theta - \Theta)$, the inelastic scattering intensity vanishes in this case, in addition to a vanishing of the elastic intensity.[4] With increasing crystal-field splitting Δ, the RIXS intensity at L_2 edge will grow as $I(L_2) \propto (\Delta/\lambda)^2$, and become comparable to that at the L_3 edge when $\Delta \simeq \lambda$.

At the L_3 edge, however, RIXS is fully allowed. The matrix elements are $B^{ff}_{\sigma\sigma} = -\sin^2\theta\ \epsilon'^*_\sigma\epsilon_\sigma - \cos^2(\theta - \Theta)\epsilon'^*_{\bar\sigma}\epsilon_{\bar\sigma} - \cos^2\theta\ \epsilon'^*_z\epsilon_z$ and $B^{ff}_{\sigma\bar\sigma} = \frac{1}{2}(-1)^\sigma \sin 2\theta\ (\epsilon'^*_{\bar\sigma}\epsilon_z - \epsilon'^*_z\epsilon_\sigma)$ for the intradoublet ones, and $B^{fg}_{\sigma\sigma} = \cos(\theta - \Theta)\sin\Theta\ \epsilon'^*_{\bar z}\epsilon_{\bar\sigma}$, $B^{fg}_{\sigma\bar\sigma} = (-1)^\sigma \cos(\theta - \Theta)\cos\Theta\ \epsilon'^*_\sigma\epsilon_{\bar\sigma}$, $B^{fh}_{\sigma\sigma} = \frac{1}{2}(-1)^\sigma[\sin 2(\theta - \Theta)\epsilon'^*_{\bar\sigma}\epsilon_{\bar\sigma} - \sin 2\theta\ (\epsilon'^*_\sigma\epsilon_\sigma - \epsilon'^*_z\epsilon_z)]$, $B^{fh}_{\sigma\bar\sigma} = -\sin^2\theta\ \epsilon'^*_z\epsilon_\sigma - \cos^2\theta\ \epsilon'^*_{\bar\sigma}\epsilon_z$ for the doublet-quartet excitations. For excitations within the $J_{\rm eff} = 1/2$ doublet, the scattering operator can be rewritten in terms of the effective angular momentum operator, which in the limit $\Delta/\lambda \ll 1$ takes the particularly simple form $D^\dagger_3 D_3 = \frac{2}{3}(\boldsymbol{\epsilon}'^*\cdot\boldsymbol{\epsilon}\ \mathbb{1} + \mathbf{P}\cdot\mathbf{J}_{\rm eff})$, where $P_x = i(\epsilon'^*_y\epsilon_z - \epsilon'^*_z\epsilon_y)$ and its cyclic permutations P_y, P_z are polarization factors. Here, the first term corresponds to elastic scattering while the $\mathbf{P}\cdot\mathbf{J}_{\rm eff}$ term gives rise to inelastic scattering.

RIXS on Sr_2IrO_4. Up to this point, the discussion is general and applies to all materials with an Ir^{4+} ion in an octahedral crystal field. Calculation of the RIXS spectra for a particular iridate is straightforward given the Hamilonian that captures the interactions between the Ir degrees of freedom. In Sr_2IrO_4 the effective low-energy Hamiltonian is obtained from the spin-orbital superexchange for the triply degenerate t_{2g} orbitals[19] by projecting it on the low-energy Kramers doublet. In the case of strong spin-orbit coupling, one finds a Heisenberg Hamiltonian for these pseudo-spin-1/2 states, with weak dipolar anisotropy due to Hund's rule coupling. The rotation of the octahedra around the z axis over an angle $\alpha \approx 11^\circ$ introduces a Dzyaloshinsky-Moriya interaction, but after an appropriate spin rotation the Hamiltonian remains of Heisenberg type.[8]

At the Ir L_3 edge, excitations within the $J_{\rm eff} = 1/2$ doublet can be described in terms of Holstein-Primakoff bosons. The single- and double-magnon intensities are, respectively,

$$
\begin{aligned}
I^{(1)} &\propto \left[\left| \frac{\sin\alpha}{\sqrt{2}} (P_x + P_y)(u_{\mathbf{q}} + v_{\mathbf{q}}) - i\, P_z (u_{\mathbf{q}} - v_{\mathbf{q}}) \right|^2 \right. \\
&\quad \left. + \frac{1}{2} \cos^2\alpha\, |P_x - P_y|^2 (u_{\mathbf{q}} - v_{\mathbf{q}})^2 \right] \delta(\omega - \omega_{\mathbf{q}}), \\
I^{(2)} &\propto \frac{1}{N} \sum_{\mathbf{k}} [\sin^2\alpha |P_x - P_y|^2 (u_{\mathbf{k}+\mathbf{q}} v_{\mathbf{k}} + u_{\mathbf{k}} v_{\mathbf{k}+\mathbf{q}})^2 \\
&\quad + \cos^2\alpha |P_x + P_y|^2 (u_{\mathbf{k}+\mathbf{q}} v_{\mathbf{k}} - u_{\mathbf{k}} v_{\mathbf{k}+\mathbf{q}})^2] \\
&\quad \times \delta(\omega - \omega_{\mathbf{k}+\mathbf{q}} - \omega_{\mathbf{k}}),
\end{aligned} \tag{3}
$$

where $u_{\mathbf{k}} = \frac{1}{\sqrt{2}} (\frac{1}{\nu_{\mathbf{k}}} + 1)^{1/2}$, $v_{\mathbf{k}} = \frac{1}{\sqrt{2}} (\frac{1}{\nu_{\mathbf{k}}} - 1)^{1/2} \,\mathrm{sign}(\gamma_{\mathbf{k}})$, $\nu_{\mathbf{k}} = \sqrt{1 - \gamma_{\mathbf{k}}^2}$, with $\gamma_{\mathbf{k}} = (\cos k_x + \cos k_y)/2$, $\omega_{\mathbf{k}} = 2J\nu_{\mathbf{k}}$ is magnon dispersion, and $\mathbf{q}$ is the reduced momentum transfer in the first Brillouin zone. A remarkable difference with L-edge RIXS on cuprates[23] is that the large spin canting, reflected in the appreciable value of α, causes the presence of spectral weight at $\mathbf{q} = \mathbf{0}$.

Transitions from $J_{\rm eff} = 1/2$ to $3/2$, which are at an energy of $\frac{3}{2}\lambda$, are expected to show a less pronounced $\mathbf{q}$ dependence. The crystal-field splitting of the quartet states

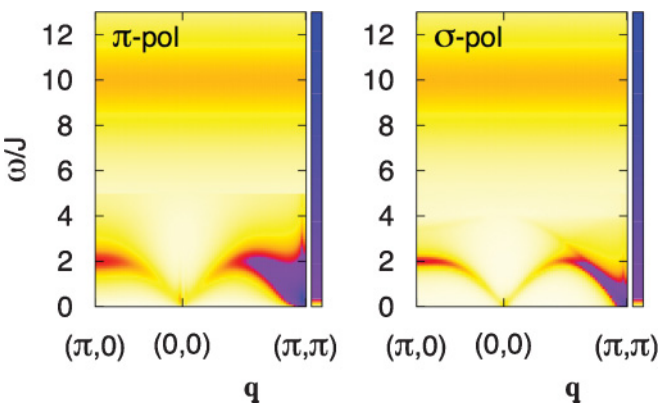

FIG. 1. (Color online) RIXS spectra of Sr_2IrO_4 at the Ir $L_3 t_{2g}$ edge. The left-hand panel shows the spectrum for incoming π polarization, and the right-hand panel for incoming σ polarization. The outgoing polarization is not measured. The intradoublet excitations are broadened by $J/2$.

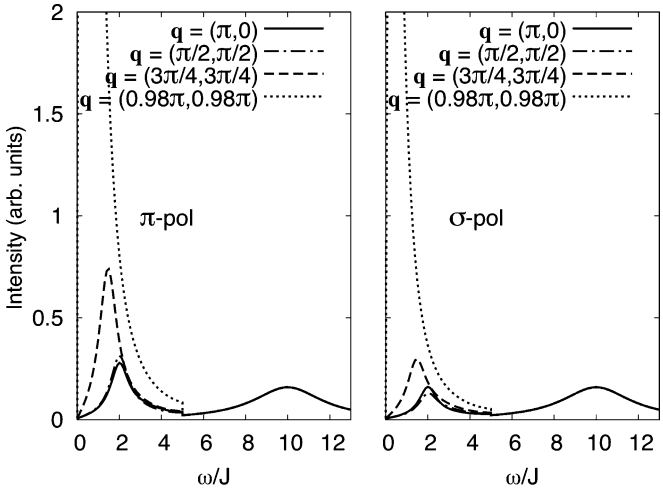

FIG. 2. Vertical cuts through Fig. 1. The left-hand panel shows spectra at several $\mathbf{q}$ for incoming π polarization, and the right-hand panel for incoming σ polarization.

in Sr_2IrO_4 is probably too small to resolve with current RIXS instruments, so we give the integrated intensity of all these excitations: $I^{(g+h)} \propto 2 + |\boldsymbol{\epsilon}' \cdot \boldsymbol{\epsilon}|^2 - |\boldsymbol{\epsilon}'^* \cdot \boldsymbol{\epsilon}|^2$. The polarization terms cancel unless both incoming and outgoing x rays are circularly polarized.

Computed RIXS spectra. We now evaluate the different contributions to the RIXS intensity. Single- and double-magnon contributions $I^{(1,2)}$ and those from the $J_{\rm eff} = 1/2$ to $3/2$ excitations $I^{(g+h)}$ are presented for the specific case of a 90° scattering angle with the scattering plane perpendicular to the IrO_2 layers. The resulting cross sections are shown in Figs. 1 and 2, where we used $\frac{3}{2}\lambda/J = 10$. In Fig. 3 the spectral weights of the different excitations are directly compared. The low-energy intradoublet excitations show a very distinct magnon dispersion, the intensity of which is strongly varying with $\mathbf{q}$. The doublet-quartet transitions with $\Delta J_{\rm eff} = 1$ are at $\frac{3}{2}\lambda$, corresponding to $\sim$0.6 eV.[20] This implies they match in energy the large spectral weight charge modes observed in optical absorption in Sr_2IrO_4.[31] Even if the local multiplet excitations are not optically active themselves, there will be mixing of the spin-orbit excited state with intersite

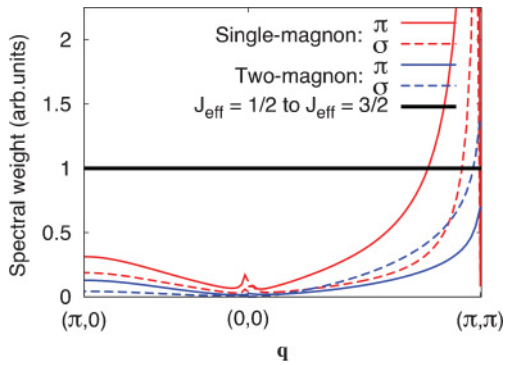

FIG. 3. (Color online) Spectral weight of different excitations. The units on the vertical axis are chosen such that the $J_{\rm eff} = 1/2$ to $3/2$ excitation has a spectral weight of unity.

charge excitations across the Mott gap. This may cause a delocalization of the doublet-quartet mode on the scale of the intersite hopping t. The dispersion- and momentum-dependent spectral weight modulations that this causes is beyond the present model calculations; here it only reflects in the use of an effective broadening of the doublet-quartet mode with t, corresponding to $\sim 4J$.

To summarize, we have determined the effective scattering operators for direct RIXS at the L edge of Ir^{4+} ions. In the limit of strong spin-orbit coupling, the RIXS spectral weight at the L_2 vanishes for cubic symmetry, but it is strong at the L_3 edge. Applying this to Sr_2IrO_4, we find that RIXS can map out the strongly dispersive single- and double-magnon excitations of the low-lying doublet and, in addition, the doublet-quartet excitations at an energy of $\frac{3}{2}\lambda$, which may mix with delocalized charge modes.[32] This shows that RIXS can accurately determine the material parameters λ and J of iridates and is an excellent tool to probe their low-energy elementary excitations, testing and characterizing proposed long-range order and topological phases.

We thank H. Takagi, B. J. Kim, J. H. Kim, and M. van Veenendaal for valuable discussions.

[1] Y. Tokura and N. Nagaosa, Science **288**, 462 (2000).
[2] H. A. Jahn and E. Teller, Proc. R. Soc. London A **161**, 220 (1937).
[3] K. I. Kugel and D. I. Khomskii, Sov. Phys. Usp. **25**, 231 (1982).
[4] B. J. Kim, H. Ohsumi, T. Komesu, S. Sakai, T. Morita, H. Takagi, and T. Arima, Science **323**, 1329 (2009).
[5] A. Shitade, H. Katsura, J. Kuneš, X.-L. Qi, S.-C. Zhang, and N. Nagaosa, Phys. Rev. Lett. **102**, 256403 (2009).
[6] D. Pesin and L. Balents, Nat. Phys. **6**, 376 (2010).
[7] J. Chaloupka, G. Jackeli, and G. Khaliullin, Phys. Rev. Lett. **105**, 027204 (2010).
[8] G. Jackeli and G. Khaliullin, Phys. Rev. Lett. **102**, 017205 (2009).
[9] A. Kitaev, Ann. Phys. **321**, 2 (2006).
[10] X. Wan, A. Turner, A. Vishwanath, and S. Y. Savrasov, Phys. Rev. B **83**, 205101 (2011).
[11] B.-J. Yang and Y. B. Kim, Phys. Rev. B **82**, 085111 (2010).
[12] C. Cosio-Castaneda, G. Tavizon, A. Baeza, P. de la Mora, and R. Escudero, J. Phys. Condens. Matter **19**, 446210 (2007).
[13] Y. Klein and I. Terasaki, J. Phys. Condens. Matter **20**, 295201 (2008).
[14] A. V. Powell, P. D. Battle, and J. G. Gore, Acta Crystallogr. C **49**, 852 (1993).
[15] S. Fujiyama, H. Ohsumi, S. Niitaka, T. Komesu, S. Takeshita, B. J. Kim, T. Arima, and H. Takagi (unpublished).
[16] A. Kotani and S. Shin, Rev. Mod. Phys. **73**, 203 (2001).
[17] S. J. Moon, M. W. Kim, K. W. Kim, Y. S. Lee, J.-Y. Kim, J.-H. Park, B. J. Kim, S.-J. Oh, S. Nakatsuji, Y. Maeno, I. Nagai, S. I. Ikeda, G. Cao, and T. W. Noh, Phys. Rev. B **74**, 113104 (2006).
[18] B. J. Kim, H. Jin, S. J. Moon, J.-Y. Kim, B.-G. Park, C. S. Leem, J. Yu, T. W. Noh, C. Kim, S.-J. Oh, J.-H. Park, V. Durairaj, G. Cao, and E. Rotenberg, Phys. Rev. Lett. **101**, 076402 (2008).
[19] For a review, see G. Khaliullin, Prog. Theor. Phys. Suppl. **160**, 155 (2005).
[20] O. F. Schirmer, A. Förster, H. Hesse, M. Wöhlecke, and S. Kapphan, J. Phys. C **17**, 1321 (1984).
[21] We refer to the cubic axes, parallel to neighboring Ir-Ir bonds. The z direction is perpendicular to the IrO_2 plane.
[22] J. Kanamori, Prog. Theor. Phys. **17**, 177 (1957).
[23] L. J. P. Ament, G. Ghiringhelli, M. M. Sala, L. Braicovich, and J. van den Brink, Phys. Rev. Lett. **103**, 117003 (2009).
[24] L. Braicovich, J. van den Brink, V. Bisogni, M. M. Sala, L. J. P. Ament, N. B. Brookes, G. M. De Luca, M. Salluzzo, T. Schmitt, V. N. Strocov, and G. Ghiringhelli, Phys. Rev. Lett. **104**, 077002 (2010).
[25] L. Braicovich, M. Moretti Sala, L. J. P. Ament, V. Bisogni, M. Minola, G. Balestrino, D. Di Castro, G. M. De Luca, M. Salluzzo, G. Ghiringhelli, and J. van den Brink, Phys. Rev. B **81**, 174533 (2010).
[26] M. Guarise, B. Dalla Piazza, M. Moretti Sala, G. Ghiringhelli, L. Braicovich, H. Berger, J. N. Hancock, D. van der Marel, T. Schmitt, V. N. Strocov, L. J. P. Ament, J. van den Brink, P.-H. Lin, P. Xu, H. M. Rønnow, and M. Grioni, Phys. Rev. Lett. **105**, 157006 (2010).
[27] L. J. P. Ament, M. van Veenendaal, T. P. Devereaux, J. P. Hill, and J. van den Brink, Rev. Mod. Phys. **83**, 705 (2011).
[28] J. J. Sakurai, *Advanced Quantum Mechanics* (Addison-Wesley, Boston, MA, 1967).
[29] M. O. Krause and J. H. Oliver, J. Phys. Chem. Ref. Data **8**, 329 (1979).
[30] W. Schülke, *Electron Dynamics by Inelastic X-Ray Scattering* (Oxford University Press, Oxford, UK, 2007).
[31] S. J. Moon, H. Jin, W. S. Choi, J. S. Lee, S. S. A. Seo, J. Yu, G. Cao, T. W. Noh, and Y. S. Lee, Phys. Rev. B **80**, 195110 (2009).
[32] In fact, recent Ir L_3 edge RIXS measurements (Refs. 33 and 34) on Sr_2IrO_4 reveal a strong inelastic signal at $\sim$0.6 eV.
[33] K. Ishii, I. Jarrige, M. Yoshida, K. Ikeuchi, J. Mizuki, K. Ohashi, T. Takayama, J. Matsuno, and H. Takagi, Phys. Rev. B **83**, 115121 (2011).
[34] Jungho Kim, D. Casa, M. H. Upton, T. Gog, Young-June Kim, J. F. Mitchell, M. van Veenendaal, M. Daghofer, J. van den Brink, G. Khaliullin, and B. J. Kim (unpublished).